HOLOS
ISSN 1807 - 1600

ANTIOXIDANT ACTIVITY OF SILVER NANOPARTICLES SYNTHESIZED WITH SULFATED POLYSACARIDES FROM SEAWEED *DICTYOTA MERTENSII.*

M. M. F. NEGREIROS, R. I. A. MACHADO, H. A. O. ROCHA*
Centro de Biociências, Programa de pós-graduação em Bioquímica, Universidade Federal do Rio Grande de Norte
https://orcid.org/0000-0003-2252-1221
hugo@cb.ufrn.br

Submetido 15/09/2020 - Aceito 15/02/2021
DOI: 10.15628/holos.2022.11174

ABSTRACT

Sulfated polysaccharides (SP) with high antioxidant capacity can be synthesized by seaweed. In addition, silver nanoparticles containing PS may have this activity superior to SP alone. *Dictyota mertensii* SP, in several tests carried out, did not present themselves as good antioxidants. Therefore, in the present paper, silver nanoparticles were synthesized with SP from the seaweed *D. mertensii* and their morphological characteristics and antioxidant capacity were analyzed. Thus, *D. mertensii* was collected on the beach of Maracajau (RN - Brazil), washed and submitted to proteolysis for 18 h. After centrifugation, the supernatant was subjected to precipitation with 2 volumes of methanol and the material obtained was centrifuged, dried, and called PM. Silver nanoparticles were synthesized using PM as a reducing agent, and called NM. NM formation was monitored by UV-visible spectroscopy. The morphological characteristics of PM and NM were analyzed by dynamic light scattering, scanning electron microscopy and atomic force microscopy. The antioxidant activities of PM and NM were evaluated by six different *in vitro* tests. The yield of obtaining PM was 7.26% ± 2.93, while the yield of obtaining NM was 49.0% ± 3.0. NMs had a rounded shape, size of 104.38 ± 2.17, Zeta potential of -19.15 and stability for 14 months. NM showed greater antioxidant activity than PM in all tests, except for CAT. These data indicate that NMs have a biotechnological potential as an antioxidant agent.

PALAVRAS-CHAVE: Nanotechnology; Fucans; Fucoidans; Brown seaweed; Biotechnology.

ATIVIDADE ANTIOXIDANTE DE NANOPARTÍCULAS DE PRATA SINTETIZADAS COM POLISSACARÍDEOS SULFATADOS DA ALGA *DICTYOTA MERTENSII.*

RESUMO

Algas marinhas comumente apresentam polissacarídeos sulfatados (PS) com alta capacidade antioxidante. Inclusive, estes na forma de nanopartículas de prata podem ter esta atividade potencializada. Todavia, os PS da alga *Dictyota mertensii*, em diversos testes realizados, não se apresentaram como bons antioxidantes. Portanto, no presente trabalho foram sintetizadas nanopartículas de prata com PS da alga *D. mertensii* e analisado suas características morfológicas e sua capacidade antioxidante. Para tal, a alga *D. mertensii* foi coletada na praia de Maracajau (RN - Brasil), lavada e submedida a proteólise por 18 h. Após centrifugação, o sobrenadante foi submetido à precipitação com 2 volumes de metanol e o material obtido foi centrifugado, seco e denominado PM. Nanopartículas de prata foram sintetizadas usando PM como agente redutor, e denominadas NM. A formação das NM foi acompanhada por espectroscopia de UV-visível. As características morfológicas de PM e NM foram analisadas por dispersão de luz dinâmica, microscopia eletrônica de varredura e microscopia de força atômica. As atividades antioxidantes de PM e NM foram avaliadas por seis diferentes testes *in vitro*. O rendimento de obtenção de PM foi de 7,26% ± 2,93, já o rendimento de obtenção de NM foi de 49,0% ± 3,0. As NM apresentaram formato arredondado, tamanho de 104,38 ± 2,17, Potencial Zeta de -19,15 e estabilidade por 14 meses. As NM apresentaram maior atividade antioxidante que PM em todos os testes, exceto no CAT. Estes dados indicam que as NM possuem um potencial biotecnológico como agente antioxidante.

KEYWORDS: Nanotecnologia, Fucanas, Fucoidans; Algas marrons, Biotecnologia.

HOLOS
ISSN 1807 - 1600

1. INTRODUTION

Silver nanoparticles have become the focus of compounds manipulation in order to improve their properties, as well as expand and enhance their applications in several areas such as cosmetics (Alba-Molina *et al*., 2019), biomedical (Prasath et al., 2019), materials (Aghihotri et al., 2020) and food (By et al., 2020).

The synthesis of silver nanoparticles can occur by several methods (Slepička et al. 2020). However, many of these methods use substances that may be toxic to living organisms, including humans, in addition, in some of these methods, there are complex procedures that hinder their use (Asharani *et al*., 2009; Sharma, Madhunapantula, & Robertson, 2012). Therefore, there is a search for alternative methods that are simpler and that use fewer toxic substances.

Polysaccharides are known as molecules of extremely low toxicity, and in 2012, Elsabahy and Wooley (2012) showed that nanoparticles made of polysaccharides have a feature of aggregating less and therefore being more biocompatible. In addition, it has been demonstrated that it is possible to make nanoparticles with polysaccharide-rich extracts, such as seaweed extracts, using a method that has little impact on the environment, also known as a green method or an ecofriendly method. Another important fact is that these nanoparticles also showed low toxicity (Rodriguez-Garraus et al., 2020).

Seaweeds are organisms of high nutritional value (Leandro et al., 2020) and in many Asian countries they are consumed as food (Nisizawa et al., 1987). One of the most abundant nutrients found in seweed is polysaccharides. These molecules have many applications in various industries such as hydrocolloids (Hentati et al., 2020), drugs (Mayer et al., 2013) and biotechnology (Vasconcelos, Araújo, & Santana, 2015; Farias & Araújo, 2014). Each taxon synthesizes specific polysaccharides. In the case of brown seaweed (Phaeophyta), fucans/fucoidans are mentioned, they are sulfated polysaccharides (SP) that contain residues of L-fucose, and some residues can be sulfated in one or more positions (Rocha et al., 2005). In addition, each species of seaweed synthesizes at least one exclusive type of sulfated polysaccharide, which can have different applications than the others (Rocha et al., 2005).

Sulfated polysaccharide-rich extracts are already used as a food additive and they have several pharmacological activities (Fiton et al., 2019). For example, Costa et al. (2010) showed SP-rich extract obtained from the seaweed *Dictyota mertensii* had antioxidant activity in different tests. However, in this paper, the activities of these extracts were considered moderate. One way to enhance the activity of these extracts would be to use them as raw material for the synthesis of silver nanoparticles.

Thus, in this study, silver nanoparticles were synthesized with SP-rich extract from the brown seaweed *D. mertensii* (Martius) Kützing using an ecofriendly method. These nanoparticles were morphologically characterized and evaluated as antioxidant agent.

2. METHODOLOGY.

2.1. Materials

Potassium ferricianyde, ferrous sulfate II, trichloroacetic acid, and sulfuric acid were purchased from Merck (Darmstadt, Germany). Nitro Blue Tetrazolium (NBT), monosaccharides, diaminoethanetetraacetic acid (EDTA), ascorbic acid, methionine, 3-(4,5-dimethylthiazolyl-2)-2,5-diphenyltetrazolium bromide (MTT), pyrocatechol violet, riboflavin, and ammonium molybdate were purchased from Sigma-Aldrich Co. (St. Louis, MA, USA). Sodium bicarbonate, non-essential amino acids, and phosphate buffered saline (PBS) were purchased from Invitrogen Corporation (Burlington, ON, Canada).

The mature seaweeds (15–30 cm long) were collected at Maracajau Beach (Rio Grande do Norte, Brazil—5°40'16" S/35°31'8.8" W). They were cleaned to eliminate residues, encrusted organisms, and epiphytes and taken to the laboratory (Laboratório de Biotecnologia de Polímeros Naturais, Departamento de Bioquímica, Universidade Federal do Rio Grande do Norte, RN). The seaweed was then identified based on its morphology. The seeweeds were washed, dehydrated, crushed, and stored protected from light and heat until the moment of use. The material collection occurred under the authorization of the Brazilian National System of Management of Genetic Heritage and Associated Traditional Knowledge SISGEN n° A72AD2B.

2.2. Methods

2.2.1. Extraction of polysaccharides

The dry seaweed was then powdered and treated with 2 volumes of ethanol (99.5%, Sigma-Aldrich Co., St. Louis, MA, USA) overnight 5 times to reduce the amount of pigments in the sample, as previously described (Dietrich et al., 1995). The supernatant was eliminated, and the power was dried at 50 °C under ventilation. The dilapidated dried material was then packed in polyethylene bags and stored at room temperature in the dark.

Approximately 5 g of dilapidated and powdered alga was suspended with four volumes of 0.25 M NaCl and the pH was adjusted to 8.0 with NaOH. Next, 75 mg of Prolav 750 alkaline protease mixture (Prozyn Biosolutions, São Paulo, SP, Brazil) was added for proteolytic digestion and the solution was incubated for 24 h at 60 °C under agitation and periodical pH adjustments. The mixture was then filtered through a cheesecloth and the obtained soluble sulfated polysaccharides were precipitated with two volumes of ice-cold methanol. After 24 h, the polysaccharides were collected using centrifugation (10,000 × g, 20 min), vacuum dried, suspended in distilled water, and analyzed. These sulfated polysaccharides from *D. mertensii* were then called PM. For the evaluation of the yield of obtaining the sulfated polysaccharides, 100% was established for the mass of dehydrated seaweed.

2.2.2. Nanoparticle Synthesis

Nanoparticle were synthesized according to a method previously described (Dipankar & Murugan, 2012). Briefly, solutions of PM (10 mg/mL) were added to a silver nitrate solution (1 mM in ultrapure water) at a proportion of 1:9 and left to rest. to determine the day on which the largest number of nanoparticles could be obtained, the absorbance of the nanoparticle suspension was monitored from 350 to 600 nm for 15 days. Then, the material obtained on day 7 (when there was

no more increase in absorption) was centrifuged twice (11500 × g, 20 min, 4 °C), suspended in ultrapure water and lyophilized. The precipitate obtained was of SP-coated silver nanoparticles (NM). To determine the yield of NM synthesis, the amount of SP-rich extract used in this synthesis was established as 100%.

2.2.3. Nanoparticle Characterization

The dynamic light scattering (DLS) measurement and the zeta potentials of the samples were performed at 25 °C on a Zeta Potential Analyzer (Brookhaven, New York, NY, USA). Briefly, NM suspensions (0.5 mg/mL in ultrapure water, pH 7.1) were analyzed in three independent experiments (n = 10), and the reported values correspond to mean ± SD.

The NM stability was evaluated by DLS. Briefly, a NM suspension (0.5 mg/mL) was prepared and stored in the dark at 4 °C for 14 months. Measurements were made every thirty days as described earlier. In addition, we also observed color change, visual aggregation, and precipitate formation.

Atomic force microscopy (AFM) was performed by a Scanning Probe Microscope (SPM) 9700 (Shimadzu, Kyoto, Japan), at the Scanning Electron Microscopy Laboratory (LABMEV), in the Department of Engineering Materials (DEMat), of Universidade Federal do Rio Grande do Norte (UFRN). Briefly, a drop of nanoparticle solution was placed on a cover slip, this material was dried under reduced pressure and the cover slip was placed on the microscope. At least 3 images were taken in different fields. All images were evaluated for the shape of the samples.

NM was processed and analyzed by SEM (*Transmission* electron microscopes *Penta FET® Precision* – OXFORD Instruments) at Centro de Tecnologia do Gás e Energias (CTGás), Natal, RN, Brazil. Briefly, 20 µL of NM suspension (0.5 mg/mL) was loaded onto a carbon-coated copper grid without gold coating and air-dried for 10 min under vacuum. The grid chamber was then placed in the SEM room and incubated in the dark at 10–20 °C for 2 h. One representative image of three independent experiments is shown.

2.2.4. Evaluation of antioxidant activity

Total Antioxidant Capacity (TAC) - This assay is based on the reduction of Mo (VI) to Mo (V) by samples and subsequent formation of a green phosphate/Mo (V) complex at an acidic pH. Tubes containing samples and the reagent solution (0.6 M sulfuric acid, 28 mM sodium phosphate, and 4 mM ammonium molybdate) were incubated at 95 °C for 90 min. After the incubation, the mixture was cooled to room temperature and the absorbance of each solution was measured at 695 nm against a blank (Costa *et al*., 2010). The total antioxidant capacity was expressed as vitamin C-equivalent.

2,2-difenil-1-picrilhidrazil (DPPH) scavenging assay. In the test, the sample's ability to donate electrons to the radical DPPH is verified (ALVES et al., 2010), with the reduction of DPPH, this reagent acquires yellow color and intensity its color can be measured by spectrophotometer at 517 nm. The greater the ability to donate electrons from the sample, the lower the staining intensity. The test was carried out at room temperature and protected from light.

Superoxide radical scavenging assay. This assay was based on the capacity of sample to inhibit the photochemical reduction of nitro blue tetrazolium (NBT) in the riboflavin-light-NBT system. Each 3 mL of reaction mixture contained 50 mM phosphate buffer (pH 7.8), 13 mM methionine, 2 mM riboflavin, 100 mM EDTA, NBT (75 mM), and 1 mL sample solution. After the production of blue formazan, the absorbance increase was determined at 560 nm after 10 min illumination from a fluorescent lamp. The entire reaction assembly was enclosed in a box lined with aluminum foil. Identical tubes with the reaction mixture were kept in the dark and served as blanks. Gallic acid was used as a positive control.

Hydroxyl radical scavenging assay. The scavenging activity of sample against the hydroxyl radical was investigated using the Fenton's reaction ($Fe^{2+} + H_2O_2 \rightarrow Fe^{3+} + OH^- + OH$). These results were expressed as an inhibition rate. Hydroxyl radicals were generated using 3 mL sodium phosphate buffer (150 mM, pH 7.4), which contained 10 mM $FeSO_4 \cdot 7H_2O$, 10 mM EDTA, 2 mM sodium salicylate, 30% H_2O_2 (200 mL), and varying sample concentrations. In the control, sodium phosphate buffer replaced H_2O_2. The solutions were incubated at 37 °C for 1 h, and the presence of the hydroxyl radical was detected by monitoring absorbance at 510 nm. Gallic acid was used as a positive control.

The ferrous-ion-chelating ability of the samples was investigated using the following methodology: Samples at different concentrations were introduced to the reaction mixture, which contained $FeCl_2$ (0.05 mL, 2 mM) and ferrozine (0.2 mL, 5 mM). The mixture was shaken and incubated for 10 min at room temperature and the absorbance of the mixture was measured at 562 nm against a blank. EDTA was used as a positive control.

To determine the ability of sample to chelate copper ions we used a previously described method (Megías *et al*., 2009). Pyrocatechol violet associates with cations, including aluminum, copper, bismuth, and thorium. In the presence of chelating agents, this association is not formed, resulting in a less intense color change. Different concentrations of the samples (0.1–2.0 mg/mL), pyrocatechol violet (4 mM), and copper II sulfate pentahydrate (50 µg/mL) were mixed in a 96-well plate and the absorbance was measured at 632 nm. EDTA was used as a positive control.

2.2.5. *Statistical Analysis*

All data are expressed as average ± standard deviation. Statistical analysis was performed using one-way ANOVA. Student-Newman-Keuls post-tests were carried out for multiple group comparisons. In all cases, $p < 0.05$ was considered statistically significant. Statistical analysis was performed using GraphPad Prism 5.01 (GraphPad Software Inc., La Jolla, CA, USA).

3. RESULTS AND DISCUSSION

3.1. Yield and analysis by UV-visible spectroscopy

The yield of obtaining PM was 7.26% ± 2.93. This value was higher than that obtained with the red seaweed *Gracilaria birdiae*, which in this case was 3.93% (Medeiros, 2015). On the other hand, it was smaller than that observed with the brown seaweeds *Spatoglossum schröederi* and *Dictyopteris justii*, which were 18.66 and 36.83%, respectively (Negreiros, 2015). This type of

HOLOS
ISSN 1807 - 1600

variation has already been observed by other authors and some factors are mentioned that cause this fact, among them the extraction method, seasonality, environmental factors, and species of the seaweed (Grosso et al., 2015).

The yield of obtaining NM was 49.0 ± 3.0. This was much higher than that observed by Medeiros (2015), who in the case, working with a SP-rich extract from the seaweed *G. birdiae*, obtained a yield in the synthesis of silver nanoparticles of only 4.25%. On the other hand, Negreiros (2015) obtained a yield of 75.5% when he made silver nanoparticles with SP extract from the seaweed *Sargassum filipendula*. We have not identified any other paper in which nanoparticles were synthesized with SP-rich extracts from seaweed and the yield of this synthesis has been demonstrated. According to Rodríguez-León et al. (2013) the quantity of silver nanoparticles obtained can be explained by the reducing power of each extract, the greater the reducing power of the extract, the greater the amount of nanoparticles obtained. Therefore, the yield of nanoparticles mentioned here varied from each seaweed due to the properties of the reducing agent (in this case, the sulfated polysaccharide of seaweed) present in the extracts.

The nanoparticle synthesis process was followed with the use of a spectrophotometer in the region from 350 to 600 nm. The formation of NM with PM was accompanied by spectroscopy, because according to Gurunathan et al. (2013) the incidence of light in the reduced silver promotes their excitation, which forms a layer called the plasmon surface. This layer promotes the deviation of light, and therefore, this deviation can be detected (from 250 to 600 nm). An increase in the values of optical density (OD) at 403 nm region is pointed out by Islam & Mukherjee (2011) as an indicator of the increase in the amount of nanoparticles in suspension. Therefore, this wavelength range was used to verify the time required for the synthesis of nanoparticles with sulfated polysaccharide from seaweed. The region shorter than 350 nm is characteristic of free silver in solution.

Figure 1A shows the NM light absorption profile. Figure 1B shows an increase in the absorbance value over the days, especially in the region that corresponds to the 403 nm length. In that region, the OD values recorded on the first day corresponded to 0.750 and increased to a value of 2,000 and 2,200 on the sixth and seventh days, respectively. Thereafter, the values remained constant until the fifteenth day, the last day of analysis of the NM light absorption profile.

It is worth noting that the increase observed in the absorption of light over time (Figure 1B) was similar to that reported during the synthesis of other silver nanoparticles, such as those synthesized under agitation with the use of the natural polysaccharide from the gum from the plant *Cyamopsis tetragonaloba* (Pandey, Goswami, & Nanda, 2012), fungi exopolysaccharides (Chen, Yan, & Wu, 2015) and sulfated polysaccharides extracted from seaweed (El-Rafie, El-Rafie, & Zahran, 2013). Another evidence of the formation of nanoparticles was found by changing the color of the suspension from light yellow to dark brown (data not shown).

HOLOS
ISSN 1807 - 1600

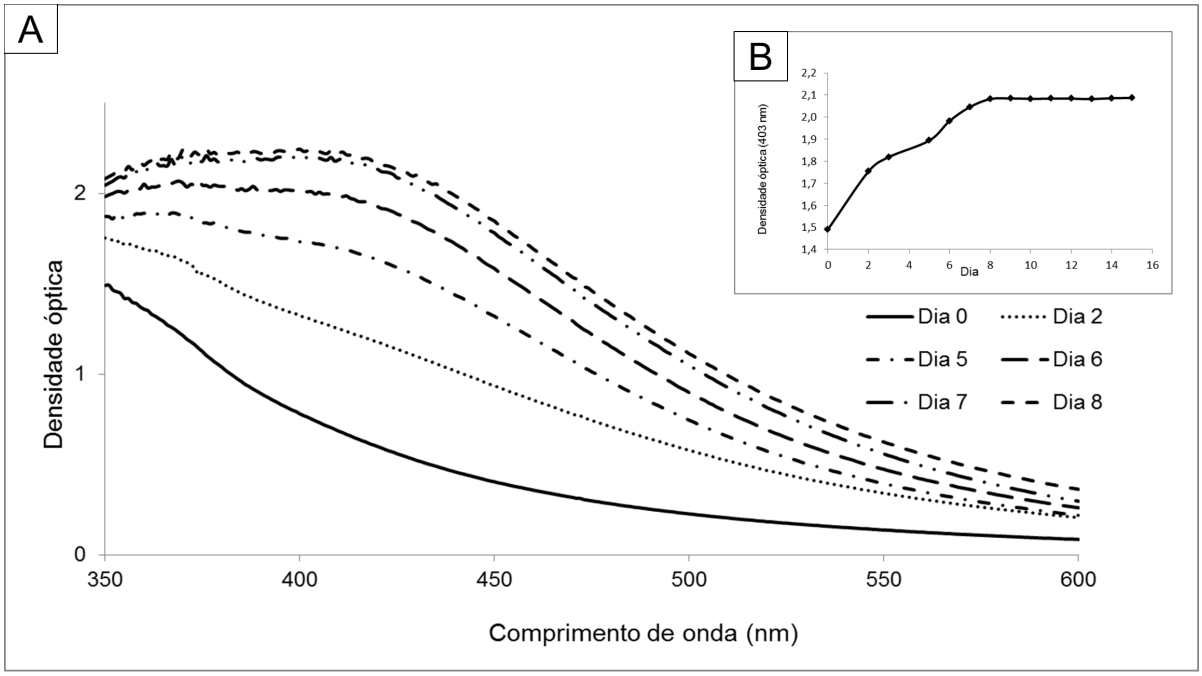

Figure 1: Light absorption profile of *D. mertensii* nanoparticles (A) Light absorption profile, scanning from 350 to 600 nm, of *D. mertensii* nanoparticles. (B) Light absorption profile, in the 403 nm region, of *D. mertensii* nanoparticles. Measured on days: Zero, two, five, six, seven and eight (from their synthesis). In the upper right corner, the increase in absorption over time.

3.2. Structural characterization of nanoparticles

3.2.1. Scanning electron microscopy

Scanning electron microscopy (SEM) and atomic force microscopy images are shown in figure 2. In both techniques, the nanoparticles are observed with a spherical shape. This geometry is already known for several silver nanoparticles (Okafor et al., 2013; Gurunathan et al., 2013). Silver nanoparticles can be amorphous or take on different geometric shapes (Mikhailov et al., 2019). Regarding nanoparticles made with SP from seaweed, for the best that we know, the only geometric shape identified so far was the spherical shape. This leads to the proposal that silver nanoparticles containing polysaccharides assume exclusively a spherical shape.

The fact that nanoparticles with polysaccharides always assume a spherical shape is a positive point, since nanoparticles rounded in are less cytotoxic compared to other shapes, such as, for example, triangular (Pal, Tak, & Song, 2007, Rodriguez-Garraus et al., 2020). Thus, it is expected that the NM in this study is also low toxic.

HOLOS
ISSN 1807 - 1600

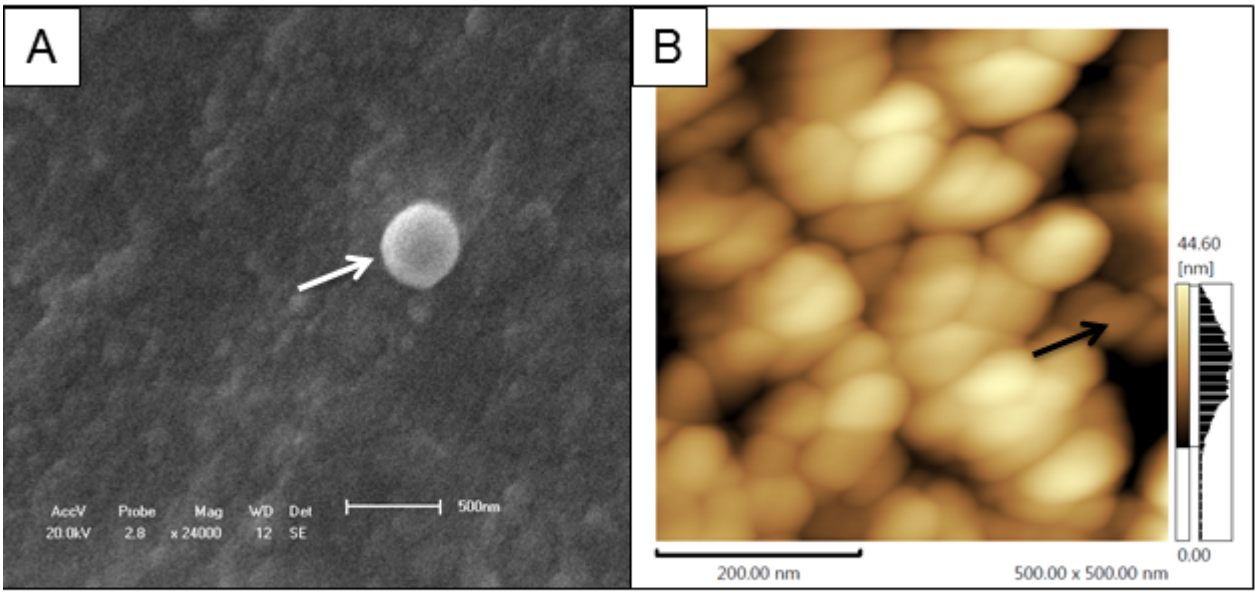

Figura 2: Scanning electron microscopy (A) and atomic force microscopy (B) of nanoparticles synthesized with sulfated polysaccharides from D. mertensii. The arrow indicates the nanoparticle. of the nanoparticle..

3.2.2. Size, stability, and zeta potential

Using dynamic light scattering (DLS) analyzes, NM was characterized by medium size and organized into populations. In addition, PM had its size measured in order to compare it with NM. The PM size was 1009.91 ± 55.5 and the NM size was 104.38 ± 2.17. It is possible to identify that there was a reduction in the size of the polysaccharides by about 10 times when in the form of nanoparticles. It should be noted that papers that cite the size of algal polysaccharides did not use DLS, therefore, this is the first one to present this method to obtain this data.

Comparing the NM size with other nanoparticles containing polysaccharides, it was found that the size of NM was like that of silver nanoparticles (120 nm) synthesized by Chen, Yan and Wu (2015). Coradeghini et al. (2013) and Rodriguez-Garraus et al. (2020) report that exceedingly small nanoparticles (> 20 nm) can present great cytotoxicity compared to larger nanoparticles. On the other hand, large nanoparticles are not easily absorbed by tissues, making it difficult to act on their respective target (Elsabahy & Wooley, 2012). Thus, according to these authors, nanoparticles with sizes 20-200 nm are particularly suitable for possible *in vivo* applications, and for some cases, as application of drugs to the liver, nanoparticles with sizes up to 500 nm can also be used. As NM are close to this size range, it is expected that they are also suitable for *in vivo* applications.

Still regarding the identification of NM sizes, it was also found that NM had three populations of varying sizes, however most of the nanoparticles (87.8%) were grouped into a predominant population. The different sizes of nanoparticles can be explained, as the extracts have different polysaccharides that vary in size, load, and biological activities, as shown by a study of Costa et al. (2010). The interactions between charges are the main factor for the structure of the nanoparticles, thus, differences in the composition and quantity or position of the charges, in the same extract, can result in variations in the size of the nanoparticles. Therefore, in the same extract there can be variations in polysaccharides that result in variations in the size of the nanoparticles. However, the predominance of one population shows a homogeneity in the nanoparticles obtained here. This fact

is not so common, as, for example, in the paper by El-Rafie, El-Rafie and Zahran (2013) there is a description of silver nanoparticles containing seaweed polysaccharides that were so different in size that it was possible to group them in at least five distinct populations.

Thus, the fact that a greater amount of nanoparticles with similar sizes have been synthesized leads to the idea that there is a type of SP that predominates in PM. This is also a positive factor for the nanoparticles synthesized here, as it is believed that the biological activities attributed to NM would be dependent mainly on the nanoparticle synthesized from this polysaccharide that is found in greater quantity, which in short, would provide greater safety in use. of NM.

The size of the nanoparticle was also periodically measured for a total period of fourteen months. The average size of NM did not change significantly, and it was found that NM remained stable during this period. Regarding the stability of other nanoparticles containing polysaccharides, stability of 25 days was found for silver nanoparticles with chitosan and sulfated L-fucose-rich polysaccharide (Huang & Li, 2014), two months for nanoparticles containing fungi exopolysaccharides (Chen, Yan, & Wu, 2015), three months for bimetallic gallic acid nanoparticles (Mittal, Kumar, & Banerjee, 2014), six months for silver nanoparticles with seaweed polysaccharides (El-Rafie, El-Rafie, & Zahran, 2013), and twelve months for silver nanoparticles containing xylan (Viana et al., 2020). As we did not find any article that showed silver nanoparticles with stable polysaccharides for more than twelve months, we believe that NM's stabilities are the most extensive ever described.

In nanoparticles, two regions are distinguished, the inner and outer regions, and the interaction of the nanoparticles with the environment occurs from the outer layer, which gives these particles different properties, including charge. The Zeta Potential is a numerical representation that points to the total charge unit (electronic potential) of the particle surface.

The zeta potential of PM and NM were -19.18 and -19.15, respectively. There was no statistically significant change between these samples. The negative charge conferred to NM also occurs for nanoparticles with sulfated polysaccharides synthesized in other papers. Venkatpurwar and Pokharkar (2011) synthesized silver nanoparticles with algal polysaccharides with a negative zeta potential of - 35.05 mV. These authors indicate that SP are responsible for this load. Chauvierre and collaborators (2003) also obtained nanoparticles of sulfated polysaccharides with negative surface charge (around - 45 mV), these authors still report that nanoparticles with dextran (neutral polysaccharide) had less negative charge (around -15 mV) compared silver nanoparticles made with heparin and sulfated dextrans. Thus, it is speculated, as occurred for Chauvierre and collaborators (2003), that the negative charge of NM is probably related to the presence and exposure of sulfate groups of PM.

Another fact about the negative charge of NM is that it may have been an important factor for good stability for fourteen months. This is because, in the aqueous system, negative or positive charges conferred to the nanoparticles contribute to the repulsion between them, preventing their aggregation and consequently preventing their instability (Ostolska & Wisniewska, 2014).

3.3. Evaluation of antioxidant activity

3.3.1. Total antioxidant capacity and DPPH radical scavenging

Several researches investigate biological activities of sulfated polysaccharides, one of these activities is the antioxidant capacity. Antioxidants can act against reactive oxygen species by several mechanisms, in the three main stages that include electron donation; ion chelation; and sequestration of free radicals (Melo, 2013). To verify the effect of NM in these different stages and compare them with PM, different tests for antioxidant activity were performed.

The activities of the Total Antioxidant Capacity (CAT) tests and the 2,2-diphenyl-1-picrilhhydryl (DPPH) radical scavenging test are summarized in Table 1. There was no statistically significant difference between PM and NM in the CAT test, thus, the formation of NM maintained the activity found for PM. Zhang et al. (2010) suggest that CAT may be related to the presence and availability of electrons in the hydroxyl groups of the sugar residues. Therefore, it is believed that the conformations assumed by the PMs in the nanoparticles allow the availability of hydroxyls so that they exercise this antioxidant activity and therefore, the CAT of the NMs was similar to that of PM.

In the DPPH tests, there were statistically significant differences between NM and PM. Therefore, the formation of nanoparticles increased the efficiency of polysaccharides as scavenging agents for reactive species, since a smaller amount of NM, consequently SP, was necessary to obtain the same radical scavenging value verified with PM.

This activity potentiating effect was also observed when nanoparticles were made of chitosan-fucoidan by Huang & Li (2014), these nanoparticles showed higher scavenging activity than free polysaccharides. However, the authors do not explain the reason for this enhancement. With the data presented here, we believed that the potentializing occurred due to the type of conformation that the polysaccharides assumed when associating silver during the formation of the nanoparticle, this conformation would be more efficient in scavenging radicals than that assumed by the polysaccharides when they are free in aqueous solution. It is hoped that in the future, with the acquisition of new data, it will be possible to confirm or not this hypothesis.

Tabel 1: Total antioxidant capacity (CAT) at a concentration of 1.0 mg/mL expressed in ascorbic acid equivalent (mg/g) and e DPPH scavenging capacity (DPPH) at a concentration of 0.25 mg / mL. * indicates significant difference between PM and NM. (P <0.05).

	CAT	DPPH
PM	41 ± 1,8	73,2 ±
NM	41,2 ± 3,7	95,1 ± *

3.3.2. Hydroxyl and superoxide Radical Scavenging Activity

Using the superoxide radical scavenging test, the samples' ability to scavenging this radical was verified. The superoxide radical scavenging activity of PM was close to 40% at a concentration of 50 µg/mL, reaching about 70% at a concentration of 500 µg/mL (Figure 3). Comparing PM with

HOLOS
ISSN 1807 - 1600

NM it is observed that in all concentrations, the activity of NM was statistically higher than the activity of PM, thus indicating that the formation of nanoparticles potentiated the activity of polysaccharides.

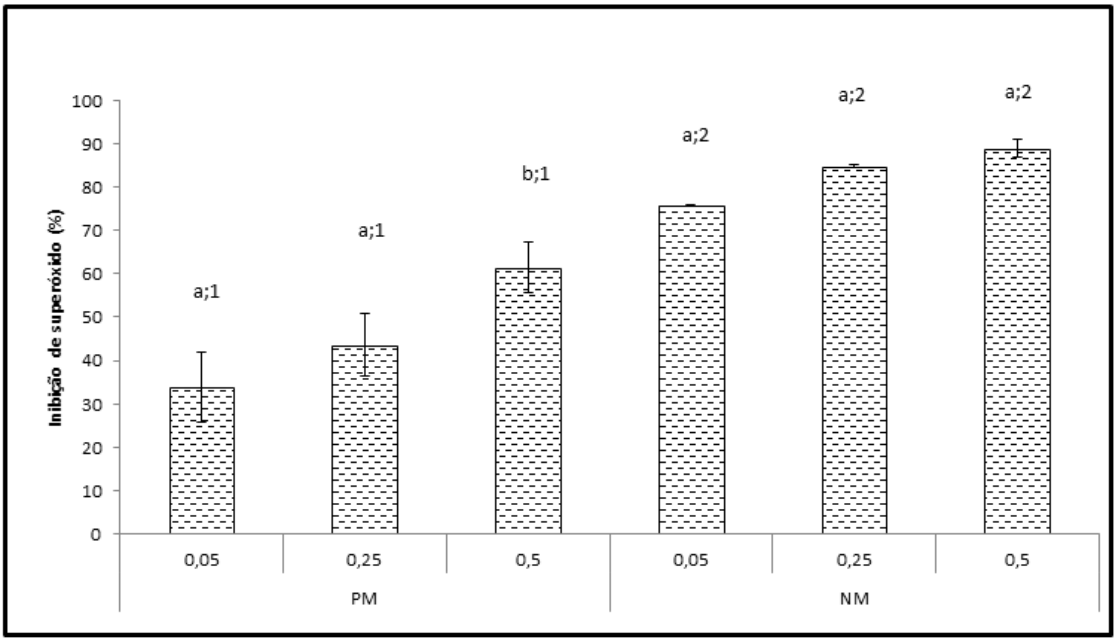

Figure 3. Superoxide radical scavenging capacity of the samples in concentrations of 0.05; 0.25 and 0.5 mg/mL. Different letters represent a significant difference between PM or NM in different concentrations; different numbers represent significant difference between PM and NM of the same concentration (P <0.05).

Using the hydroxyl radical scavenging assay, the ability of the samples to scavenger this radical was analyzed.

In Figure 4, low activity is observed for all samples, with a maximum of 6.08% for NM in a concentration of 2 mg/mL. The hydroxyl radical scavenging activity did not increase with increasing PM concentration, but increased with increasing NM concentration. It is also possible to notice that there are higher values of activity in NM when compared to the respective PM, again indicating an increase in activity with the formation of nanoparticles.

As discussed above, this effect of potentiating radical scavenging was observed by Huang and Li (2014), and it is believed that the potentiation of the activities evaluated occurred due to the type of conformation that the polysaccharides assumed when associating with silver during the formation of the nanoparticle making it more efficient at scavenging radicals.

HOLOS
ISSN 1807 - 1600

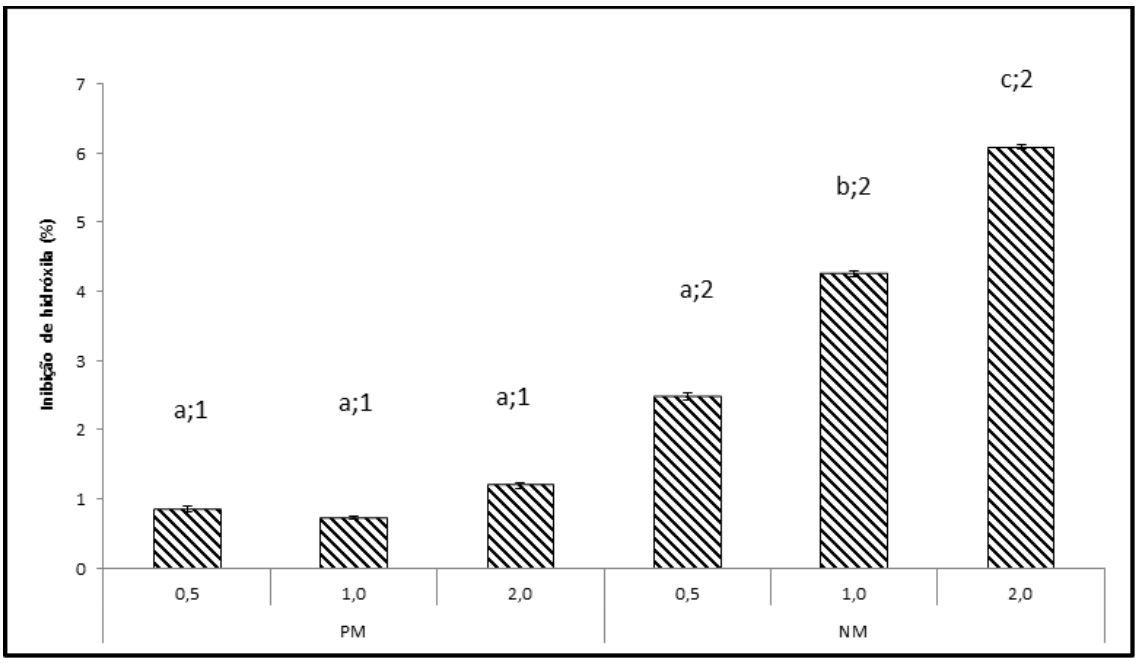

Figure 4: Hydroxyl radical scavenging capacity of the samples in concentrations of 0.05; 0.25 and 0.5 mg/mL. Different letters represent a significant difference between PM or NM in different concentrations; different numbers represent significant difference between PM and NM of the same concentration (P <0.05).

3.3.3. Ferric and cupric chelating capacity

Another strategy to prevent the harmful effect of hydroxyl radicals is through the chelating action of metals (Zou et al., 2008). This is because, according to Ueda et al. (1996), metal ions participate in the process of generating these radicals. Iron and copper ions occur in large quantities in organisms and the neutralization of their effects is of great relevance for the normal functioning of cells (Drouin et al., 1996), therefore, the ability of samples to chelate these ions was evaluated. (Figures 5 and 6).

The ferric chelating ability test measures the ability of the sample to compete with ferrozine for iron. Using this assay, the ability of the samples to chelate this ion was verified. In Figure 5, it is observed that the values of percentage of iron chelation of PM and NM. It shows that the PM activities are lower for the concentration of 0.1 mg/mL (22.3%) and higher for the concentrations of 2.0 mg/mL (75.5%).

Relating the PM and NM it is observed in the highest concentration tested there is a significant difference in the concentrations of 1.0 and 2.0 mg/mL, therefore, the formation of NM also potentiated the metal chelating activity of PM.

HOLOS
ISSN 1807 - 1600

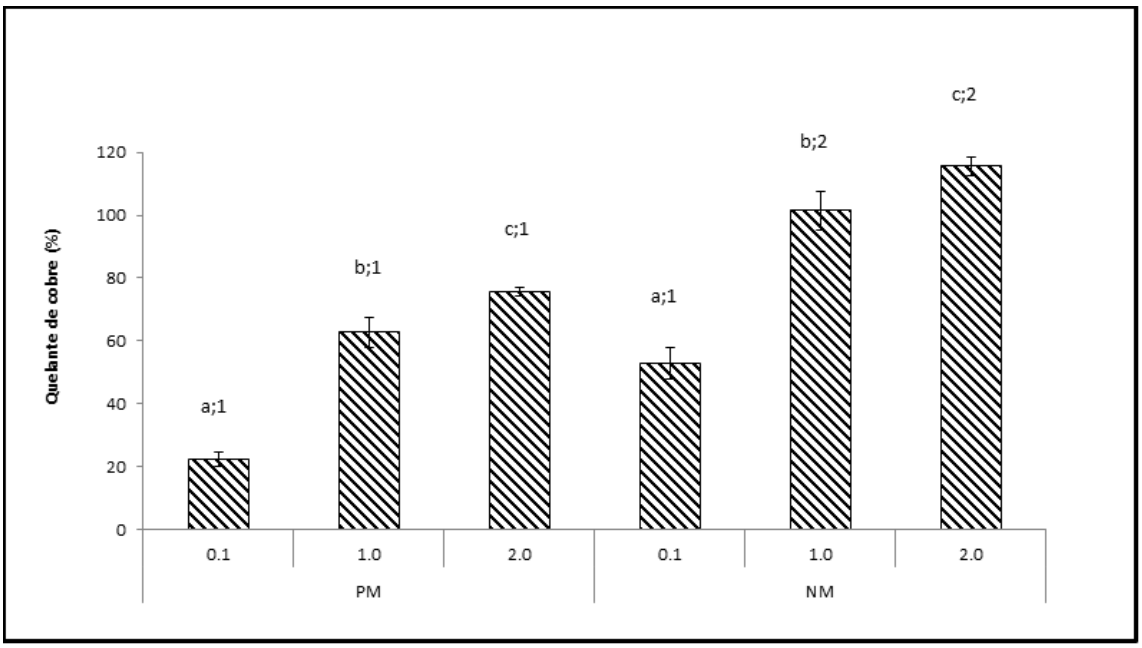

Figure 5: Ferric chelating capacity of samples in concentrations of 0.1; 1.0; and 2.0 mg / ml. Different letters represent a significant difference between PM or NM in different concentrations; different numbers represent significant difference between PM and NM of the same concentration (P <0.05).

Using the cupric chelation test, the capacity of the samples to chelate this ion was determined (Figure 6). At the concentration of 0.5 mg/mL PM obtained 67% activity, while NM obtained 114% activity at the same concentration. This fact indicates that the activity of the nanoparticle was superior to that of the polysaccharide and the formation of NM also potentiated the cupric chelating activity of PM.

Knowing that the antioxidant effect can be enhanced when nanoparticles are formed, we sought to better understand which structural modifications would be responsible for this increase in NM activity. The main evidence of structural modification presented here in this work is the probable binding of silver to sulfate groups present in polysaccharides. Sulfate groups can be separated into two groups: those that are important for radical scavenging activity (SI), and those that are not (SN). These two types of sulfate groups occur because according to Wang and collaborators (2013) the amount of sulfate groups is not proportional to the radical scavenging activity.

It is worth noting that an SI sulfate group can be an SN sulfate group, and vice versa, depending on the conformation that the polymer assumes. Therefore, it is believed that the bonding of sulfate groups with silver led to a structural modification, which ended up exposing more SI groups, which therefore increased the sequestering activity of the nanoparticles. The same line of thought can be used for the phenomenon observed in chelation tests, that is, greater activity of nanoparticles.

HOLOS
ISSN 1807 - 1600

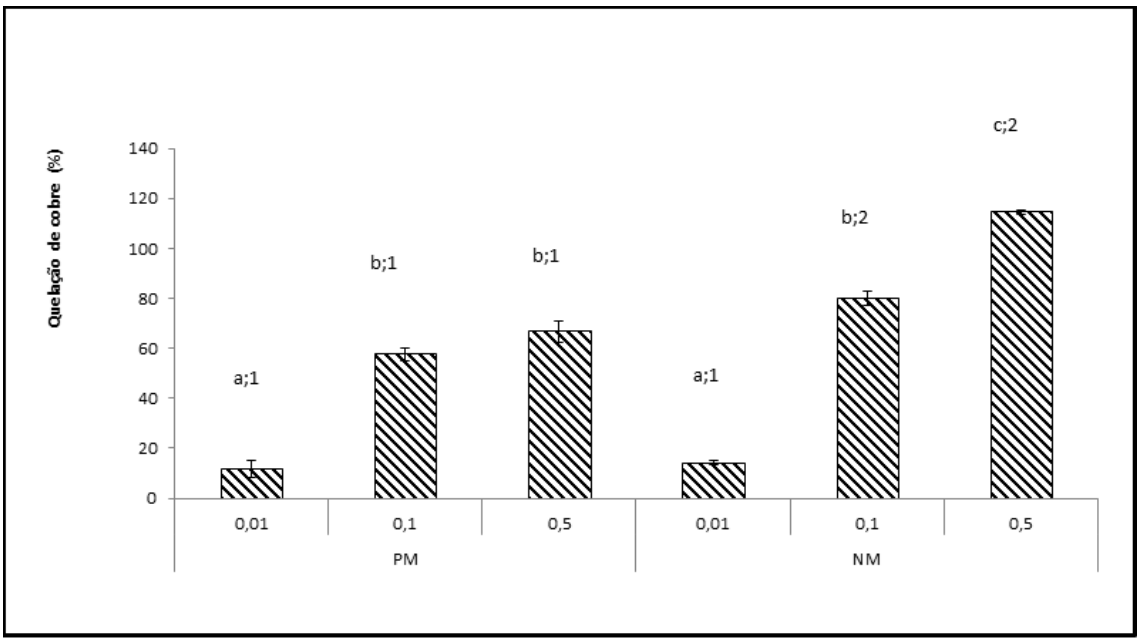

Figure 6: Cupric chelating capacity of samples in concentrations of 0.01; 0.1; and 0.5 mg/mL. Different letters represent a significant difference between PM or NM in different concentrations; different numbers represent significant difference between PM and NM of the same concentration (P <0.05).

Another important feature of NM is that they have a high stability, and this can be important so that their antioxidant activity lasts for a long time. Since Kong and collaborators (2014) point out that the less stable nanoparticles are more easily added, and therefore, they reduce the area of possible interaction with free radicals, thus reducing their antioxidant activity.

4. CONCLUSION

it was possible to synthesize silver nanoparticles with SP from *D. mertensii* using a method with little environmental impact (ecofriendly method). These nanoparticles were stable for long periods of time, have a spherical shape and small size. The rearrangement of the polysaccharides in the form of nanoparticles potentiated their antioxidant effect in the DPPH, superoxide ions, and hydroxyl radical scavenging assays, as well as ferric and cupric chelating tests. Therefore, the synthesis of nanoparticles with SP from *D. mertensii* constitutes a potentializing mechanism for their diverse biological activities.

5. ACKNOWLEDGMENTS

The authors wish to thank and Ministério de Ciência, Tecnologia, Inovações (MCTI) (Science and Technology Ministry in Brazil, in loose translation). H.A.O.R. is a CNPq fellowship-honored researcher. Marilia Negreiros and Raynara Machado are thankful for doctorate and master scholarships from CAPES. This research was presented at Programa de Pós-Graduação em BIoquímica at Universidade Federal do Rio Grande do Norte, as part of the M.Sc. thesis of Marília Negreiros. This research was funded by Conselho Nacional de Desenvolvimento Científico e Tecnológico-CNPq (n° 408369/2016-7), Coordenação de Aperfeiçoamento Pessoal de Nível Superior (CAPES), Programa Ciências do Mar (AUXPE-CIMAR-1956/2014), Programa Nacional de Cooperação Acadêmica (CAPES/PROCAD).

6. REFERÊNCIAS BIBLIOGRÁFICAS

Agnihotri, R., Gaur, S., Albin, S. (2020). Nanometals in dentistry: Applications and toxicological implications- a systematic review. *Biological Trace Element Research, 197*(1), 70-88.

Alba-Molina, D., Giner-Casares, J. J., Cano, M. (2019). Bioconjugated Plasmonic Nanoparticles for Enhanced Skin Penetration. *Topics in Current Chemistry*, *378*(1), 8.

Alves, C. Q., David, J. M., David, J. P., Bahia, M. V., & Aguiar, R. M. (2010). Métodos para determinação de atividade antioxidante in vitro em substratos orgânicos. *Quimica Nova*, *33*(10), 2202–2210.

Asharani, P. V, Low, G., Mun, K., Hande, M. P., & Valiyaveettil, S. (2009). Cytotoxicity and Genotoxicity of Silver Nanoparticle in Human Cells. *American Chemical Society*, *3*(2), 279–290.

Bi, Y., Marcus, A. K., Robert, H., Krajmalnik-Brown, R., Rittmann, B. E., Westerhoff, P., Ropers, M. H., Mercier-Bonin, M. (2020). The complex puzzle of dietary silver nanoparticles, mucus and microbiota in the gut. *Journal of Toxicology and Environmental Health, Part B,* 23(2), 69-89.

Chauvierre, C., Labarre, D., Couvreur, P., & Vauthier, C. (2003). Novel Polysaccharide-Decorated Poly (Isobutyl Cyanoacrylate) Nanoparticles. *Pharmaceutical Research*, *20*(11), 1786–1793.

Chen, X., Yan, J., & Wu, J. (2015). Characterization and antibacterial activity of silver nanoparticles prepared with a fungal exopolysaccharide in water. *Food Hydrocolloids*, 53, 1–6.

Coradeghini, R., Gioria, S., García, C. P., Nativo, P., Franchini, F., Gilliland, D., Rossi, F. (2013). Size-dependent toxicity and cell interaction mechanisms of gold nanoparticles on mouse fibroblasts. *Toxicology Letters*, *217 (3)*, 205–216.

Costa, L. S., Fidelis, G. P., Cordeiro, S. L., Oliveira, R. M., Sabry, D. a., Câmara, R. B. G., Rocha, H. a O. (2010). Biological activities of sulfated polysaccharides from tropical seaweeds. *Biomedicine and Pharmacotherapy*, *64*(1), 21–28.

Dietrich, C. P., Farias, G. G., De Abreu, L. R., Leite, E. L., Da Silva, L. F., & Nader, H. B. (1996). A new approach for the characterization of polysaccharides from algae: Presence of four main acidic polysaccharides in three species of the class Phaeophycea. *Free Radical Biology and Medicine*, *21*(3), 261–273.

Dipankar, C., & Murugan, S. (2012). The green synthesis, characterization and evaluation of the biological activities of silver nanoparticles synthesized from Iresine herbstii leaf aqueous extracts. *Colloids and Surfaces B: Biointerfaces*, *98*, 112–119.

Drouin, R., Rodriguez, H., Gao, S.-W., Gebreyes, Z., O'Connor, T. R., Holmquist, G. P., & Akman, S. A. (1996). 57. Cupric ion/ascorbate/hydrogen peroxide-induced dna damage: dna-bound copper ion primarily induces. *Free Radical Biology & Medicine, 21*(3), 261–273.

El-Rafie, H. M., El-Rafie, M. H., & Zahran, M. K. (2013). Green synthesis of silver nanoparticles using polysaccharides extracted from marine macro algae. *Carbohydrate Polymers*, *96*(2), 403–410.

Elsabahy, M., & Wooley, K. L. (2012). Design of polymeric nanoparticles for biomedical delivery applications. *Chemical Society Reviews*, *41*(7), 2545.

Farias, E. A. de O., & Araújo, T. D. S. A. (2014). Aplicações dos flavonóides em biotecnologia: propriedades terapêuticas e aplicações nanotecnológicas. *Revista Brasileira De Inovação Tecnológica Em Saúde*, 4 (2), 1–32.

Fitton, H. J., Stringer, D. S., Park, A. Y., Karpiniec, S. N. (2019).Therapies from Fucoidan: New Developments. *Marine Drugs, 17*(10), 571.

Grosso, C., Valentão, P., Ferreres, F., & Andrade, P. B. (2015). Alternative and Efficient Extraction Methods for Marine-Derived Compounds. *Mar. Drugs*, 13 (5), 3182–3230.

Gurunathan, S., Raman, J., Abd Malek, S. N., John, P. a., & Vikineswary, S. (2013). Green synthesis of silver nanoparticles using Ganoderma neo-japonicum Imazeki: A potential cytotoxic agent against breast cancer cells. *International Journal of Nanomedicine*, *8*, 4399–4413.

Hentati, F., Tounsi, L., Djomd,i D., Pierre, G., Delattre, C., Ursu, A. V., Fendri, I., Abdelkafi, S., Michaud, P. (2020). Bioactive polysaccharides from seaweeds. *Molecules, 25*(14), 3152.

Huang, Y., & Li, R. (2014). Preparation and Characterization of Antioxidant Nanoparticles Composed of Chitosan and Fucoidan for Antibiotics Delivery. *Marine Drugs*, *12 (8)*, 4379–4398.

Islam, a. K. M. M., & Mukherjee, M. (2011). Effect of temperature in synthesis of silver nanoparticles

Leandro, A., Pacheco, D, Cotas, J., Marques, J. C., Pereira, L., Gonçalves, A. M. M. (2020). Seaweed's Bioactive candidate compounds to food industry and global food security. *Life (Basel), 10*(8), E140.

Mayer, A. M. S., Rodríguez, A. D., Taglialatela-Scafati, O., & Fusetani, N. (2013). Marine pharmacology in 2009-2011: Marine compounds with antibacterial, antidiabetic, antifungal, anti-inflammatory, antiprotozoal, antituberculosis, and antiviral activities; affecting the immune and nervous systems, and other miscellaneous mechanisms. *Marine Drugs*, *11*(7), 2510–2573.

Medeiros, C. G. (2015) Síntese verde de nanopartículas de prata a partir de polissacarídeos sulfatados de *Gracilaria birdiae* e caracterização de sua atividade antioxidante. Monografia de graduação, Universidade Federal do Rio Grande do Norte - UFRN, Natal, Brasil.

Megías, E., Pastor-cavada, E., Torres-fuentes, C., Girón-calle, J., Alaiz, M., Rocio, J., Vioque, J. (2009). Chelating , antioxidant and antiproliferative activity of Vicia sativa polyphenol extracts. *Eur Food Res Technol*, *230*, 353–359.

Melo, K. R. T., Camara, R. B. G., Queiroz, M. F., Vidal, A. A. J., Lima, C. R. M., Melo-Silveira, R. F., … Rocha, H. A. O. (2013). 69. Evaluation of sulfated polysaccharides from the brown seaweed dictyopteris justii as antioxidant agents and as inhibitors of the formation of calcium oxalate crystals. *Molecules*, *18*(12), 14543–14563.

Mikhailov, O. V., Mikhailova, E. O. (2019). Elemental silver nanoparticles: biosynthesis and bio applications. *Materials (Basel), 12*(19), 3177.

Mittal, A. K., Kumar, S., & Banerjee, U. C. (2014). Quercetin and gallic acid mediated synthesis of bimetallic (silver and selenium) nanoparticles and their antitumor and antimicrobial potential. *Journal of Colloid and Interface Science*, *431*, 194–199.

Negreiros, M. M. F. (2015) Nanopartículas de prata contendo polissacarídeos sulfatados de algas: caracterização química, morfológica e identificação de suas atividades antioxidante, bactericida, antiproliferativa e imunomodulatória. Dissertação de mestrado, Universidade Federal do Rio Grande do Norte, Natal, Brasil.

Nisizawa, K., Noda, H., Kikuchi, R., & Watanabe, T. (1987). The main seaweed foods in Japan. *Hydrobiologia*, *151–152*(1), 5–29.

Okafor, F., Janen, A., Kukhtareva, T., Edwards, V., & Curley, M. (2013). Green synthesis of silver nanoparticles, their characterization, application and antibacterial activity. *International Journal of Environmental Research and Public Health*, *10*(10), 5221–5238.

Ostolska, I., & Wiśniewska, M. (2014). Application of the zeta potential measurements to explanation of colloidal Cr2O3 stability mechanism in the presence of the ionic polyamino acids. *Colloid and Polymer Science*, *292*(10), 2453–2464.

Pal, S., Tak, Y. K., & Song, J. M. (2007). Does the antibacterial activity of silver nanoparticles depend on the shape of the nanoparticle? A study of the gram-negative bacterium Escherichia coli. *Applied and Environmental Microbiology*, *73*(6), 1712–1720.

Prasath, S., Palaniappan K. (2019). Is using nanosilver mattresses/pillows safe? A review of potential health implications of silver nanoparticles on human health. *Environ Geochem Health*. *41*(5), 2295-2313.

Rocha, H. A. O., Moraes, F. A., Trindade, E. S., Franco, C. R. C., Torquato, R. J. S., Veiga, S. S., … Dietrich, C. P. (2005). Structural and hemostatic activities of a sulfated galactofucan from the brown alga *Spagtoglossum schröederi*: An ideal antithrombotic agent? *Journal BIological Chemistry*, *280*(50), 41278-41288.

Rodríguez-León, E., Iñiguez-Palomares, R., Navarro, R. E., Herrera-Urbina, R., Tánori, J., Iñiguez-Palomares, C., & Maldonado, A. (2013). Synthesis of silver nanoparticles using reducing agents obtained from natural sources (Rumex hymenosepalus extracts). *Nanoscale Research Letters*, *8*(1), 318.

Rodriguez-Garraus, A., Azqueta, A., Vettorazzi, A., López de Cerain, A. (2020). Genotoxicity of silver nanoparticles. *Nanomaterials (Basel). 10*(2), 251.

Slepička P., Slepičková, K. N., Siegel, J., Kolská, Z., Švorčík, V. (2020). Methods of gold and silver nanoparticles preparation. *Materials (Basel)*, *13*(1), 1.

Sharma, A., Madhunapantula, S. V., & Robertson, G. P. (2012). Toxicological considerations when creating nanoparticle based drugs and drug delivery systems? *Expert Opin Drug Metab Toxicol*, *8*(1), 47–69.

Ueda, J., Saito, N., Shimazu, Y., & Ozawa, T. (1996). A Comparison of Scavenging Abilities of Antioxidants against Hydroxyl Radicals. *Archives of Biochemistry and Biophysics*, *333*(2), 377–384.

Vascoscelos, A. G., Araújo, K. V. D., & Santana, L. de A. B. (2015). Polissacarídeos Extraídos De Algas Marinhas E Suas Aplicações Biotecnológicas: Uma Revisão. *Revista Brasileira De Inovação Tecnológica Em Saúde*, 27–51. Retrieved from https://periodicos.ufrn.br/reb/article/view/5898/5694

Venkatpurwar, V., & Pokharkar, V. (2011). Green synthesis of silver nanoparticles using marine polysaccharide: Study of in-vitro antibacterial activity. *Materials Letters*, *65*(6), 999–1002.

Viana, R. L. S., Fidelis, G. P., Medeiros, M. J. C., Morgano, A. M., Alves, M. G. C. F., Passero, L. F. D., Pontes, D. L., Theodoro, R. C., Arantes, T. D., Sabry, D. A., Sassaki, G. L., Melo-Silveira, R. F., Rocha, H.A.O. (2020). Green synthesis of antileishmanial and antifungal silver nanoparticles using corn cob xylan as a reducing and stabilizing agent. *Biomolecules, 10*, 1235.

Wang, J., Niu, S., Zhao, B., Wang, X., Yao, J., Zhang, J., Zhao, Y. (2013). Regioselective synthesis of sulfated guar gum: Comparative studies of structure and antioxidant activities. *International Journal of Biological Macromolecules*, *62*, 734–740.

Zhang, Z., Wang, F., Wang, X., Liu, X., Hou, Y., & Zhang, Q. (2010). Extraction of the polysaccharides from five algae and their potential antioxidant activity in vitro. *Carbohydrate Polymers*, *82*(1), 118–121.

Zou, C., Du, Y., Li, Y., Yang, J., Feng, T., Zhang, L., & Kennedy, J. F. (2008). 55. Preparation of lacquer polysaccharide sulfates and their antioxidant activity in vitro. *Carbohydrate Polymers*, *73*(2), 322–331.

COMO CITAR ESTE ARTIGO:

Fernandes-Negreiros, M. M., Machado, R. I. de A., & Rocha, H. A. O. (2022). ANTIOXIDANT ACTIVITY OF SILVER NANOPARTICLES SYNTHESIZED WITH SULFATED POLYSACARIDES FROM SEAWEED DICTYOTA MERTENSII. HOLOS, 3. Recuperado de https://www2.ifrn.edu.br/ojs/index.php/HOLOS/article/view/11174

SOBRE OS AUTORES:

HOLOS
ISSN 1807 - 1600

M.M. FERNANDES-NEGREIROS
Laboratório de Biotecnologia de Polímeros Naturais - BIOPOL, Depto. de Bioquímica, UFRN. E-mail: marilia_negreiros16@yahoo.com.br
ORCID-ID: https://orcid.org/0000-0002-5560-9687

R.I.A. MACHADO
Laboratório de Biotecnologia de Polímeros Naturais - BIOPOL, Depto. de Bioquímica, UFRN. E-mail: raynara_yusk@hotmail.com
ORCID-ID: https://orcid.org/0000-0002-3333-5128

H.A.O.ROCHA
Universidade Federal do Rio Grande do Norte. E-mail: hugo@cb.ufrn.br
ORCID-ID: https://orcid.org/0000-0003-2252-1221

Editora responsável: Francinaide de Lima Silva Nascimento
Avaliadores *Ad Hoc*: Moacir Fernandes Queiroz Neto e Vinicius Dutra Campelo

Recibido 15 de setembro de 2020
Aceito: 15 de fevereiro de 2021
Publicado: 22 de dezembro de 2022